JOURNAL OF CATALYSIS 75, 23–38 (1982)

Characterization of Supported Iridium Catalysts Prepared from $Ir_4(CO)_{12}$

KATSUMI TANAKA, KENNETH L. WATTERS, AND RUSSELL F. HOWE[1]

Laboratory for Surface Studies and Department of Chemistry, University of Wisconsin, Milwaukee, Wisconsin 53201

Received May 21, 1981; revised December 4, 1981

The characterization of silica- and alumina-supported iridium catalysts prepared from $Ir_4(CO)_{12}$ is described. The techniques employed are infrared spectroscopy, temperature-programmed desorption, and gravimetric chemisorption measurements. Supported $Ir_4(CO)_{12}$ begins to decompose on heating *in vacuo* above 75°C, and decomposition is complete at 350°C. The major product of decomposition on silica is metallic iridium, whereas on alumina a fraction of the iridium becomes oxidized. Hydrogen reduction of both silica- and alumina-supported catalysts following decomposition of the parent complex *in vacuo* produces highly dispersed metallic iridium. From observed shifts in the infrared frequencies of adsorbed CO with coverage it is concluded that the iridium may be in the form of two-dimensional rafts, containing possibly 20 atoms or more.

INTRODUCTION

Many studies have now been reported of supported metal catalysts prepared by decomposition of transition metal cluster carbonyl complexes absorbed on high-surface-area oxide supports (*1–28*). The cluster complex precursors provide in principle the possibility of preparing supported metal atom clusters of known size and shape. In practice, however, evidence for retention of the original cluster structure following adsorption of the complex and removal of the carbonyl ligands is not generally available (*19*). Nevertheless, supported metal catalysts prepared from cluster complexes show in some cases significant differences in activity from those prepared by conventional methods (*1, 4, 9–12, 16, 18, 20–22*), and an understanding of these differences is an important objective of current investigations.

The preparation of supported iridium catalysts from the complex $Ir_4(CO)_{12}$ was first reported by Anderson *et al.* (*5, 7*), and a preliminary infrared spectroscopic study of the decomposition of $Ir_4(CO)_{12}$ adsorbed on silica and alumina was described by Howe (*6*). Subsequently, Foger and Anderson (*12*) and Ichikawa and Shikakura (*22*) have investigated the catalytic activity of supported iridium prepared from $Ir_4(CO)_{12}$ for hydrogenolysis and methanation reactions, respectively.

The purpose of the present work was to further study the decomposition of $Ir_4(CO)_{12}$ adsorbed on silica and alumina supports, and to characterize the iridium catalysts so produced. The techniques employed were infrared spectroscopy, temperature-programmed desorption (TPD), and gravimetric chemisorption measurements. The results obtained are compared with literature data for conventional iridium catalysts prepared by hydrogen reduction of supported Ir(IV) (*29–34*).

EXPERIMENTAL

Catalyst Preparation

Catalyst samples were prepared by impregnation of the supports (Davison grade 62 silica gel, 340 m^2g^{-1}, or Akzo Chemie CK 300 γ-alumina, 200 m^2g^{-1}) with a cyclohexane solution of $Ir_4(CO)_{12}$. The iridium complex is only slightly soluble in cyclohexane. Refluxing for several hours gave a pale yellow solution containing up to 38 mg

[1] To whom correspondence should be addressed.

0021-9517/82/050023-16$02.00/0

of complex per 100 ml, without causing any decomposition. Such solutions containing known amounts of complex were added to the supports in air at room temperature. The supports had not been previously outgassed, and were thus fully hydroxylated. In the case of γ-alumina, $Ir_4(CO)_{12}$ was rapidly adsorbed from solution, as indicated by fading of the yellow color of the solution. The filtered catalyst was dried in air at room temperature. In contrast, no measurable adsorption occurred from solution onto the silica support. Evaporation of the solvent left crystallites of $Ir_4(CO)_{12}$ dispersed through the silica.

Catalyst samples were analyzed for iridium by atomic absorption spectrophotometry (Galbraith Laboratories) following evacuation and reduction in hydrogen at 350°C. The iridium contents of the catalyst samples used are given in Table 1. These correspond to approximately 50% of the loadings calculated from the amounts of $Ir_4(CO)_{12}$ used in the preparation, indicating significant loss of the complex through sublimation during outgassing *in vacuo*. Such sublimation is commonly observed with supported transition metal carbonyl complexes (*5*, *55*).

TABLE 1

Gravimetric CO Adsorption Data

Iridium content (wt%)	CO : Ir ratio[a] after activation	
	In vacuo[b]	In H_2[b]
$Ir_4(CO)_{12}$–SiO_2		
0.18	0.94	1.44
0.55	1.13	1.19
1.05	1.21	1.34
$Ir_4(CO)_{12}$–Al_2O_3		
0.23	0.84	1.30
0.25	1.00	1.74
0.66[c]	0.50	0.71
1.34	0.69	1.32

[a] Irreversibly adsorbed CO-to-total Ir ratio.
[b] At 350°C.
[c] Aged sample.

Temperature-Programmed Desorption

TPD measurements were carried out in a dynamically pumped glass system with a base pressure below 5×10^{-5} Torr. About 0.5 g of catalyst was placed in a glass bucket centered in a cylindrical tube. Decomposition of the fresh catalysts was measured by first evacuating at room temperature, then raising the temperature of a furnace surrounding the sample tube at a constant rate of 1.5°K min^{-1}. Gases evolved were analyzed with a quadrupole mass filter (Molytek Spectromass 80) located between the sample and the pumps. Such measurements are qualitative only; unless otherwise stated the CO and CO_2 evolved were measured with the same mass filter sensitivity, but no attempt was made to calibrate the instrument in absolute terms. TPD measurements of adsorbed CO were conducted similarly, following adsorption of CO at room temperature.

Gravimetric Adsorption Measurements

A vacuum microbalance (Cahn RG-HV) was used to measure CO adsorption on the iridium catalysts. Approximately 0.5 g of catalyst was employed in each experiment. Uptake of CO was found to reach equilibrium at room temperature and 5 Torr within 30 min. The irreversibly adsorbed CO was taken to be that remaining on the catalyst after prolonged evacuation at room temperature.

Infrared Spectra

Infrared spectra were obtained from pressed wafers of catalyst in a vacuum cell of conventional design which permitted heat treatment up to 400°C in a furnace section. A Nicolet MX1 Fourier transform spectrophotometer was employed. Spectra were accumulated at a resolution of 2 cm^{-1} for typically 5 min. (160 scans). Where necessary, background spectra of the support oxides were subtracted.

RESULTS

Temperature-Programmed Desorption

TPD curves for the decomposition of silica- and alumina-supported $Ir_4(CO)_{12}$ *in vacuo* are shown in Fig. 1. The evolution of CO and CO_2 is plotted versus temperature (the quadrupole mass filter used does not detect H_2). Freshly prepared $Ir_4(CO)_{12}$–SiO_2 and $Ir_4(CO)_{12}$–Al_2O_3 gave similar TPD curves (Figs. 1a and b, respectively) which were independent of the iridium content over the range 0.18 to 1.34 wt% Ir. The CO evolution showed a single sharp maximum at about 160°C, followed by a broad continuous evolution possibly peaking at 300–350°C. The CO peak at 160°C was accompanied by a CO_2 peak (in the case of $Ir_4(CO)_{12}$–Al_2O_3 the CO_2 peak is superimposed on a lower-temperature peak due to CO_2 evolution from the Al_2O_3 support). Further CO_2 evolution occurred above 300°C.

TPD curves for an aged $Ir_4(CO)_{12}$–Al_2O_3 sample (exposed to air for approximately 1 year following preparation) are shown in Fig. 1c. In this case, CO and CO_2 were evolved together on heating above 50°C, but no well-defined peaks were observed. Similar curves were obtained from freshly prepared $Ir_4(CO)_{12}$–Al_2O_3 samples which were deliberately exposed to H_2O at its room-temperature saturation vapor pressure, suggesting that reaction with adsorbed water may be responsible for the modified behavior of aged samples. These effects were not investigated further; all subsequent experiments with $Ir_4(CO)_{12}$–Al_2O_3 employed freshly prepared samples. No aging effects were observed with $Ir_4(CO)_{12}$–SiO_2.

TPD curves for CO adsorbed on an Ir–SiO_2 catalyst prepared by decomposition of $Ir_4(CO)_{12}$ at 350°C *in vacuo* are shown in Fig. 2a. There was an almost continuous evolution of CO over the temperature range 50–350°C. A small CO_2 peak occurred around 120°C, and further evolution of CO_2 was observed above 300°C. Almost identical TPD curves were obtained for CO adsorbed on Ir–SiO_2 catalysts which had been reduced in H_2 at 350°C following decomposition of $Ir_4(CO)_{12}$ *in vacuo* at 350°C (Fig. 2b).

TPD curves for CO adsorbed on Ir–Al_2O_3 catalysts are shown in Fig. 3. Catalysts prepared by decomposition of $Ir_4(CO)_{12}$ *in vacuo* at 350°C gave a continuous evolution of CO and CO_2 together on heating above 50°C (Fig. 3a). Ir–Al_2O_3 samples which had been reduced in H_2 following decomposition *in vacuo* at 350°C, on the other hand, gave TPD curves for adsorbed CO similar to those for Ir–SiO_2 catalysts (Fig. 3b). The curves in Figs. 3c and d were obtained by adsorbing CO to saturation coverage at 25°C on a reduced Ir–Al_2O_3 catalyst, then evacuating at 180 or 210°C, respectively, prior to cooling to 25°C and beginning the TPD measurement.

Gravimetric Adsorption Measurements

The results of gravimetric CO adsorption measurements on various silica- and alumina-supported iridium catalysts prepared from $Ir_4(CO)_{12}$ are summarized in Table 1. The data are presented as the ratios CO (irreversibly adsorbed): Ir. Blank experiments established that there was no irreversible CO adsorption on the catalyst supports under the conditions used here. With the exception of an aged alumina-supported sample, all catalysts which had been reduced in H_2 at 350°C adsorbed more than one CO per iridium. The CO uptakes after H_2 reduction were significantly higher than those after activation *in vacuo* for the alumina-supported catalysts, whereas for silica-supported catalysts only the lowest-loading sample (0.18 wt% Ir) showed an increased CO uptake following H_2 reduction.

Infrared Spectra

Infrared spectra in the carbonyl stretching region of silica-supported $Ir_4(CO)_{12}$ are shown in Fig. 4. In all cases the spectrum of the silica support has been subtracted. The

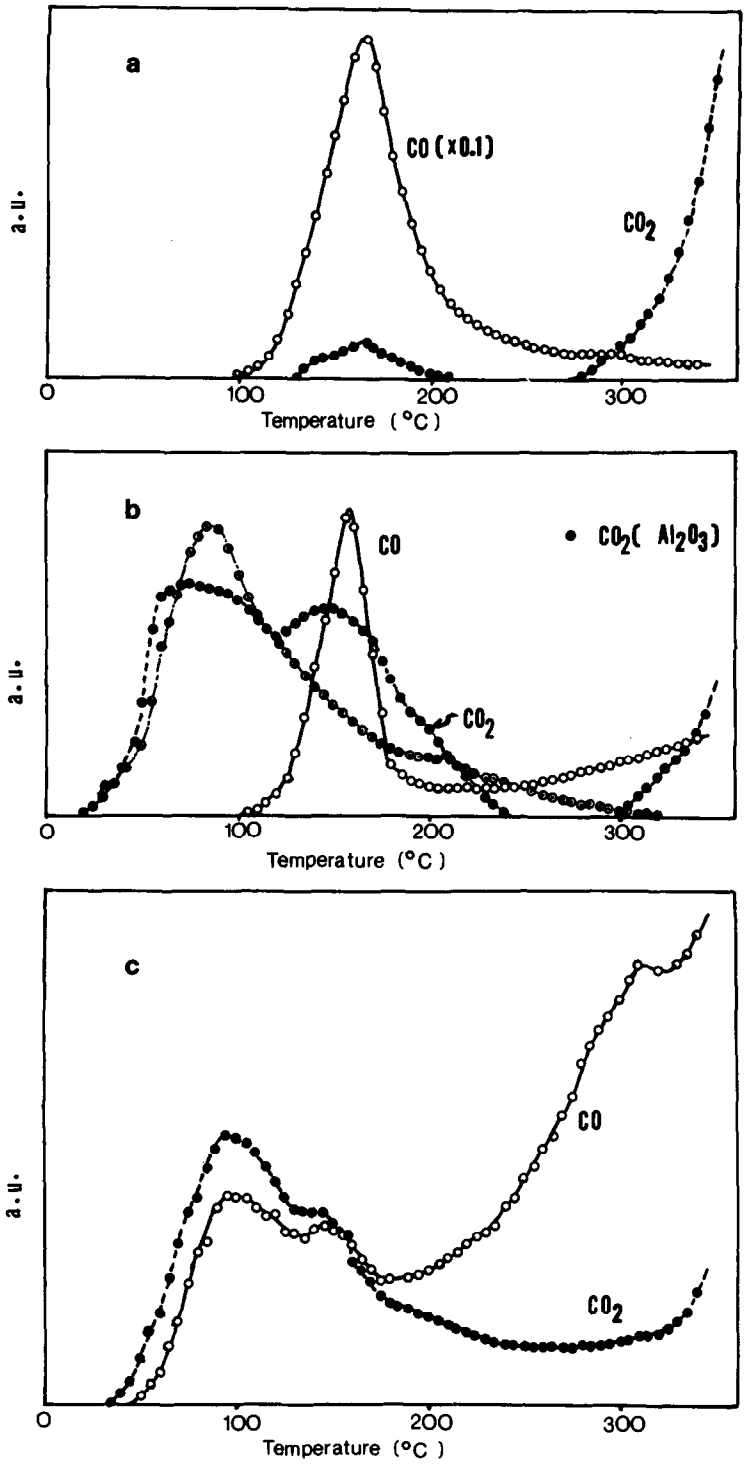

FIG. 1. TPD curves for the decomposition of silica- and alumina-supported $Ir_4(CO)_{12}$ *in vacuo* (vertical scale is in arbitrary units). (a) $Ir_4(CO)_{12}$ on silica (1.05 wt% Ir); (b) on alumina (0.25 wt% Ir, ⊙ denotes CO_2 desorption from the alumina support alone); (c) "aged" alumina-supported sample (see text).

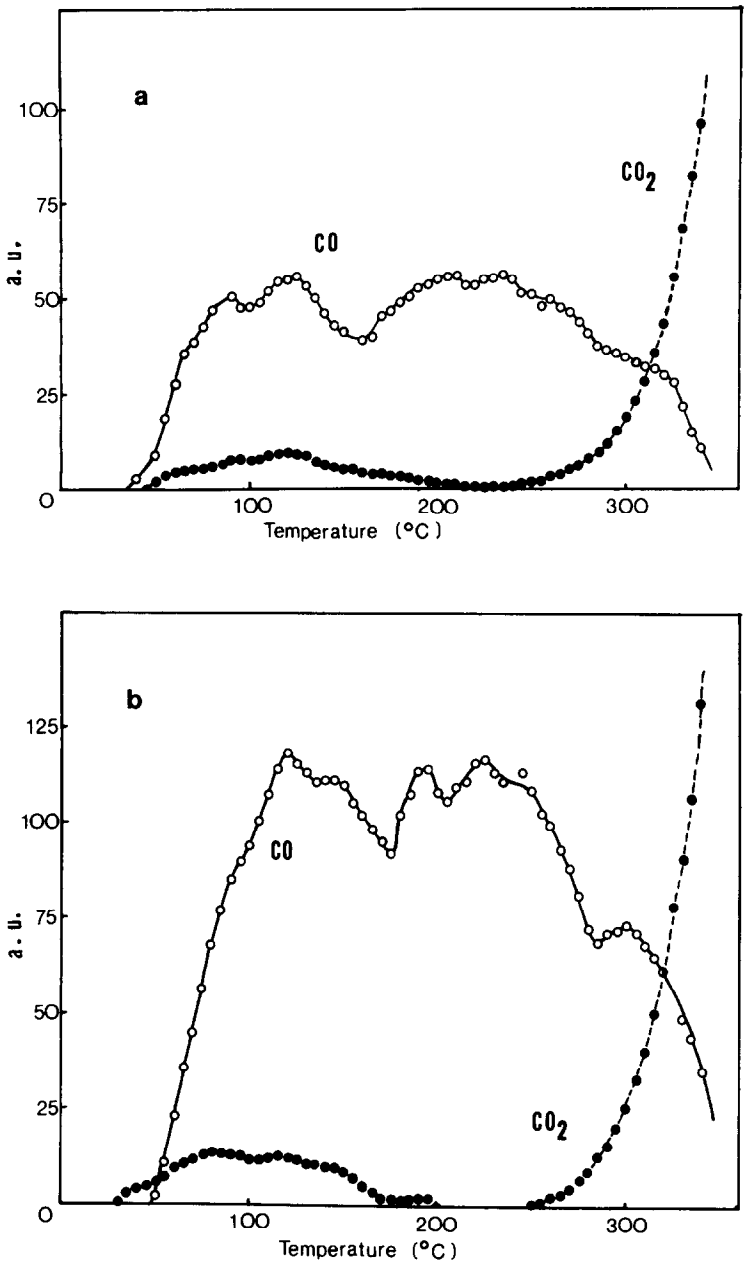

FIG. 2. TPD curves for CO adsorbed on Ir–SiO_2 catalysts prepared by (a) decomposition of $Ir_4(CO)_{12}$ *in vacuo;* (b) decomposition *in vacuo* followed by H_2 reduction.

freshly prepared catalyst (1.05 wt% Ir) in air or after evacuation at room temperature has no absorption bands in this region, but showed an intense negative absorption at 2123 cm^{-1} (Fig. 4A). This feature was removed completely after evacuation at 100°C, and replaced by an intense positive absorption band at 2054 cm^{-1}, with shoulders at 2086 and 2008 cm^{-1} (Fig. 4B). Evacuation at successively higher temperatures caused a gradual reduction in the intensity of the 2054-cm^{-1} band and a shift to lower

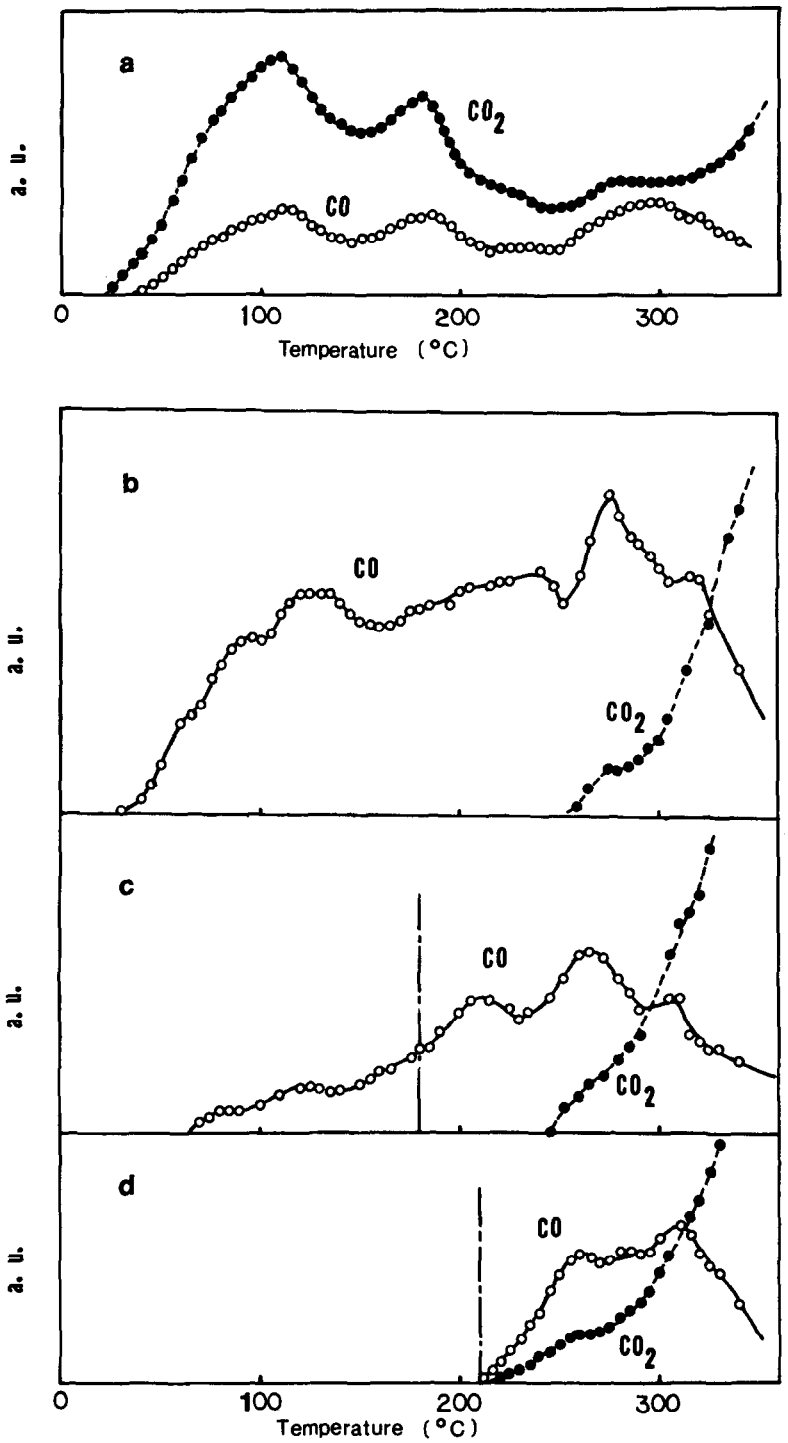

FIG. 3. TPD curves for CO adsorbed on Ir–Al_2O_3 catalysts. (a) Catalyst prepared by decomposition of $Ir_4(CO)_{12}$ *in vacuo;* (b)–(d) decomposition followed by H_2 reduction, sample evacuated at 25, 180, and 210°C, respectively, prior to beginning TPD.

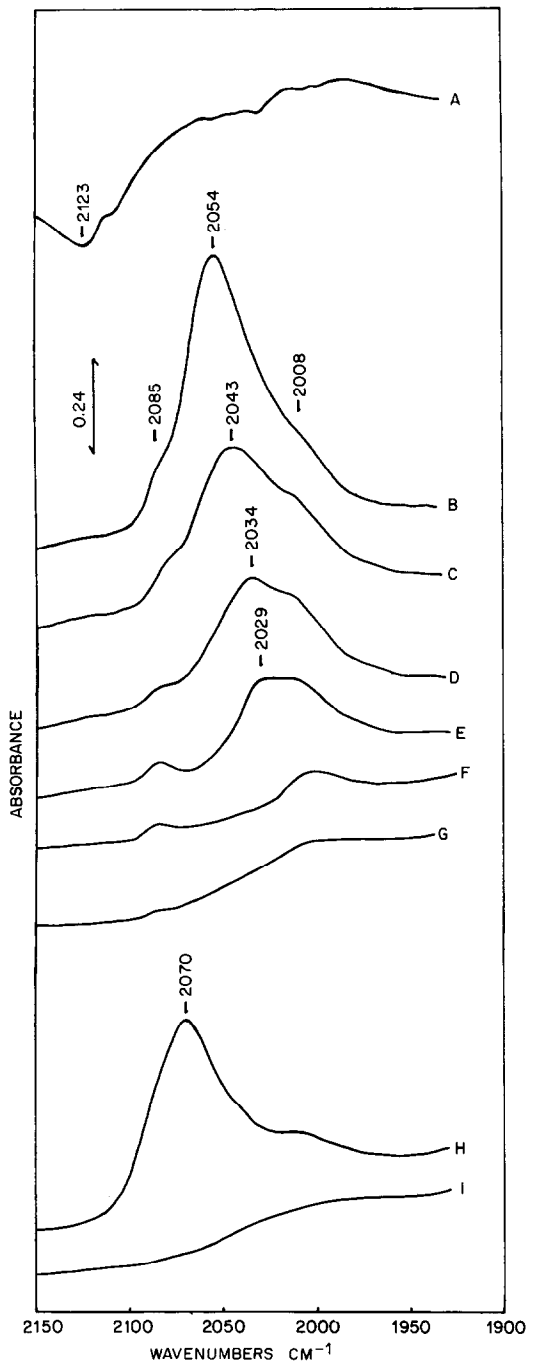

FIG. 4. Infrared spectra of decomposition of $Ir_4(CO)_{12}$ on silica. (A) Catalyst as prepared in air; (B) evacuated at 100°C for 1 hr; (C) 150°C; (D) 200°C; (E) 250°C; (F) 300°C; (G) 350°C; (H) CO adsorbed at room temperature (I) reduced in H_2 at 350°C.

frequency. After evacuation at 300°C (Fig. 4F) only the 2086- and 2008-cm^{-1} bands remained, and these were almost completely removed at 350°C (Fig. 4G). Subsequent exposure to CO gave an intense band at 2070 cm^{-1}. Similar spectra were obtained from $Ir_4(CO)_{12}$–SiO_2 samples containing 0.5 wt% Ir, but reproducible difference spectra in the carbonyl region could not be obtained for the lowest-loading samples (0.18 wt%).

Figure 5 shows spectra obtained following CO adsorption on an Ir–SiO_2 catalyst prepared by decomposition of $Ir_4(CO)_{12}$ *in vacuo* followed by H_2 reduction at 350°C. Initial adsorption of CO produced an intense single band at 2066 cm^{-1} (Fig. 5A). On subsequent evacuation at successively higher temperatures this band decreased in intensity and shifted to lower frequency. Evacuation at 350°C was necessary to remove all adsorbed CO (the sloping baseline in Fig. 5G is due to imperfect subtraction of a band due to the silica support in this region). Further adsorption of CO completely restored the 2066-cm^{-1} band.

Figure 6 shows the results of an experiment in which a 1 : 1 mixture of ^{12}CO and ^{13}CO was adsorbed on a hydrogen-reduced Ir–SiO_2 sample. Adsorption of the mixture at room temperature produced a broad single band at about 2042 cm^{-1} with a lower-frequency shoulder (Fig. 6A). Outgassing at 100 and 200°C (Figs. 6B, C) shifted the band to lower frequency and increased the relative intensity of the lower-frequency shoulder.

Figure 7 shows spectra obtained during decomposition of $Ir_4(CO)_{12}$ adsorbed on alumina (1.34 wt% Ir). The spectrum of the freshly prepared catalyst in air was unchanged on evacuation at room temperature or 50°C for 1 hr (Fig. 7A). After 1 hr at 100°C, however, three new bands appeared in the carbonyl region (Fig. 7B) at 2069, 2039, and 1997 cm^{-1}. Exposure to CO at this point did not restore the original spectrum. The 2039-cm^{-1} band was removed after 1 hr at 150°C (Fig. 7C); evacuation at higher temperatures caused a gradual re-

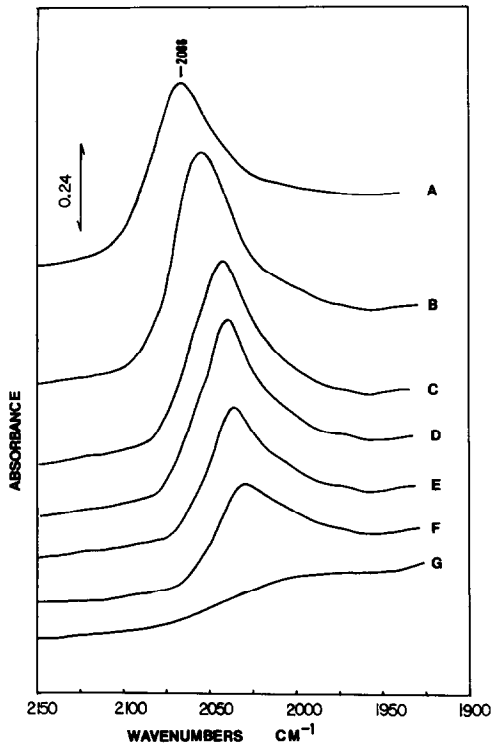

FIG. 5. Infrared spectra of CO adsorbed on reduced Ir–SiO_2. (A) CO adsorbed to saturation coverage at 25°C; (B) evacuated at 100°C for 1 hr; (C) 150°C; (D) 200°C; (E) 250°C; (F) 300°C; (G) 350°C.

duction in the intensity of the remaining bands. After 1 hr at 350°C, the 2069- and 1995-cm^{-1} bands were almost completely removed; subsequent exposure to CO at room temperature did not restore the original spectrum, but gave rise to a new band of moderate intensity around 2065 cm^{-1} (Fig. 7G). Similar spectra were obtained during decomposition of $Ir_4(CO)_{12}$ on catalysts containing lower iridium loadings.

CO adsorption on a hydrogen-reduced Ir–Al_2O_3 catalyst (1.34 wt% Ir) gave the spectra shown in Fig. 8. The single broad band at 2063 cm^{-1} shifted progressively to lower frequency as CO was removed by evacuation above room temperature, and all adsorbed CO was removed after 3 hr at 350°C. The spectrum obtained by adsorbing a ^{12}CO : ^{13}CO mixture on a similar sample is shown in Fig. 6D. CO adsorption on hydrogen-reduced catalysts containing lower loadings of iridium (0.25 or 0.66 wt%) produced an additional pair of bands at 2086 and 2016 cm^{-1}.

DISCUSSION

Decomposition of $Ir_4(CO)_{12}$

Thermogravimetric measurements by Psaro *et al.* (*35*) have shown that unsupported $Ir_4(CO)_{12}$ decomposes in the temperature range 170–220°C, producing CO and metallic iridium. In contrast, evolution of CO from silica- and alumina-supported $Ir_4(CO)_{12}$ begins at 100°C (at a heating rate comparable to those used in (*35*)). The TPD curves for silica- and alumina-supported $Ir_4(CO)_{12}$ are remarkably similar, considering the differences between the catalysts as prepared. The decomposition of the complex evidently does not depend on whether it is molecularly adsorbed from solution (on

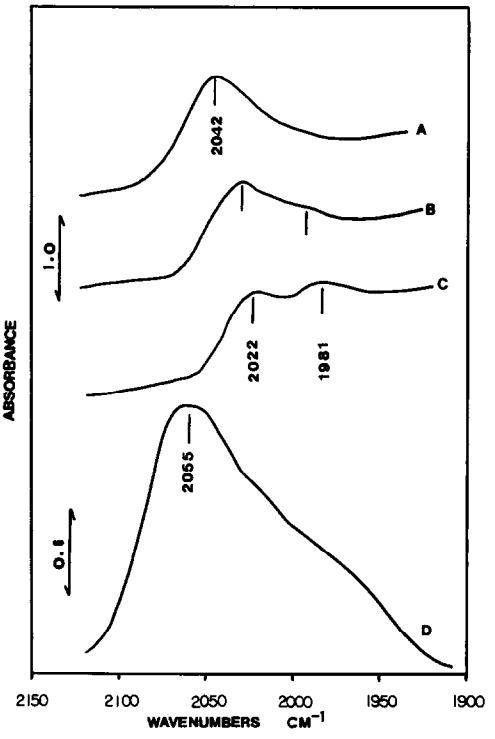

FIG. 6. Infrared spectra of a 1 : 1 ^{12}CO : ^{13}CO mixture adsorbed (A) on reduced Ir–SiO_2; (B) evacuated at 100°C; (C) 200°C for 1 hr; (D) on reduced Ir–Al_2O_3.

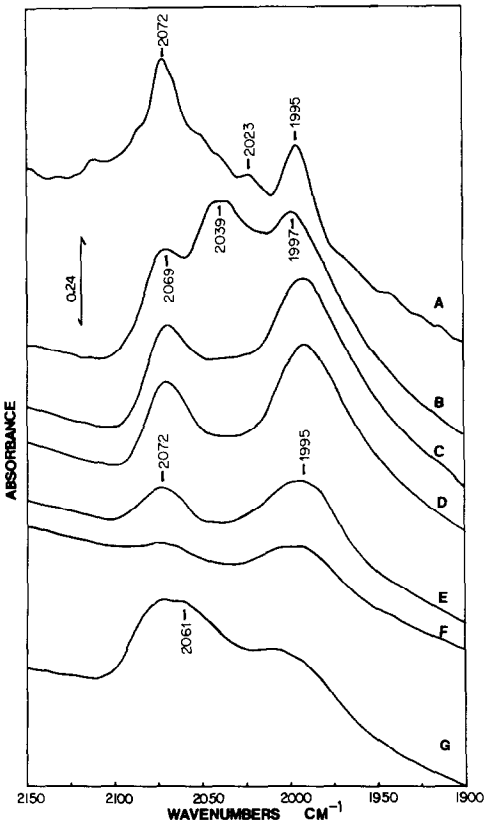

FIG. 7. Infrared spectra of decomposition of $Ir_4(CO)_{12}$ on alumina. (A) catalyst as prepared, in air; (B) evacuated at 100°C for 1 hr; (C) 150°C; (D) 200°C; (E) 300°C; (F) 350°C; (G) CO adsorbed at room temperature.

alumina) or impregnated in the form of small crystallites by evaporation of the solvent (on silica). Furthermore, Hucul and Brenner (*26*) have recently reported a TPD curve (in flowing helium) for $Ir_4(CO)_{12}$ on Al_2O_3 prepared by dry mixing the complex and the support in the absence of solvent which closely resembles the curves obtained in this work (the CO peak maximum is shifted about 50°C to higher temperature in (*26*) as a result of the faster heating rate employed). It may thus be concluded from TPD experiments that the decomposition of supported $Ir_4(CO)_{12}$ is insensitive to the method of preparation, and the nature of the support.

In contrast, the infrared spectra of silica- and alumina-supported $Ir_4(CO)_{12}$ show significant differences. As noted previously (*6*), the spectrum of freshly prepared $Ir_4(CO)_{12}$–Al_2O_3 closely resembles that of solid $Ir_4(CO)_{12}$ (*36*), although the improved resolution in this work reveals some differences in the relative intensities of the lower-frequency bands (Table 2). The 2072- and 2033-cm^{-1} bands of $Ir_4(CO)_{12}$ on alumina are assigned to the two T_2 infrared-active carbonyl stretching modes which are observed in both the solid-state and solution spectra of $Ir_4(CO)_{12}$. The third band, observed in the solid but not in solution, was attributed by Abel *et al.* (*36*) to the T_1 mode which is infrared inactive in exact T_d symmetry, but which becomes active on a slight distortion from T_d toward overall D_{2d} symmetry in the solid. On the alumina surface, further distortion may be expected, increas-

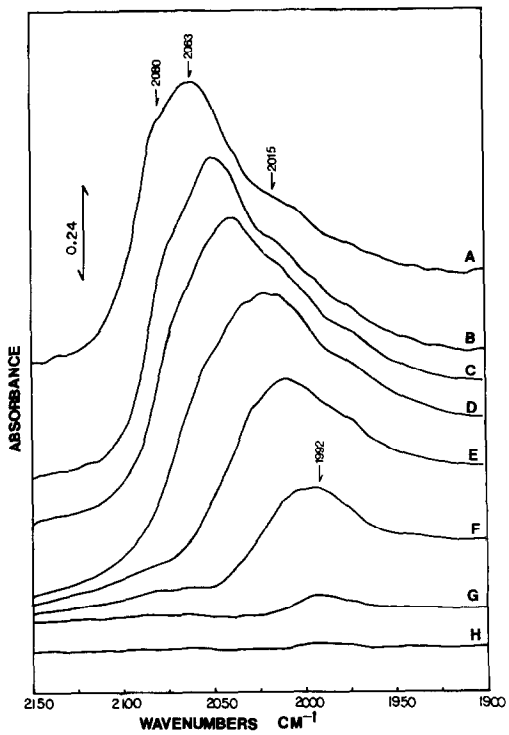

FIG. 8. Infrared spectra of CO adsorbed on reduced Ir–Al_2O_3. (A) CO adsorbed to saturation coverage at 25°C; (B) evacuated at 50°C for 1 hr; (C) 100°C; (D) 150°C; (E) 250°C; (F) 300°C; (G) 350°C for 1 hr; (H) 350°C for 3 hr.

TABLE 2

Infrared Frequencies

Parent complex	
$Ir_4(CO)_{12}$ solid[a]	2066(s) 2030(2) 2005(m)
$Ir_4(CO)_{12}$ solution[a]	2071 2032
$Ir_4(CO)_{12}$ on Al_2O_3	2072(s) 2023(m) 1995(s)
Species observed during decomposition	
$Ir(CO)_2$ on SiO_2	2080 2008
$Ir(CO)_2$ on Al_2O_3	2070 1995
$(Ir)_nCO$ on SiO_2	2054 → 2029[b]
$(Ir)_nCO$ on Al_2O_3	2040 → 2020[b]
Species observed after CO adsorption	
$(Ir)_nCO$ on SiO_2	2066 → 2010[b]
$(Ir)_nCO$ on Al_2O_3	2065 → 1995[b]
$(Ir)_n(CO)_2$ on Al_2O_3	2086 2019[c]

[a] Ref. (*36*).

[b] Band shifts to lower frequency with decreasing coverage.

[c] Resolved only in low-loading samples.

ing the intensity of the T_1 band relative to the T_2 bands. The intense negative absorption in the spectrum of freshly prepared $Ir_4(CO)_{12}$–SiO_2 samples is due to anomalous scattering of radiation in the vicinity of the carbonyl bands by small crystallites of solid $Ir_4(CO)_{12}$ (the Christiansen effect (*37*)). This is removed when samples are heated to a sufficiently high temperature (75–100°C) to cause volatilization of the solid and subsequent interaction with the support. In this temperature range, however, decomposition of the adsorbed complex has already begun, so that a clean spectrum of $Ir_4(CO)_{12}$ adsorbed in silica could not be obtained.

Decomposition of adsorbed $Ir_4(CO)_{12}$ at 100°C or higher temperatures produced similar features in the spectra of both silica- and alumina-supported catalysts; a pair of bands of approximately equal intensity (at 2080 and 2008 cm^{-1} on alumina) which were gradually reduced in intensity on outgassing at successively higher temperatures, and a single band (initially at 2054 cm^{-1} on silica and 2040 cm^{-1} on alumina) which decreased in intensity and shifted to lower frequency on outgassing at higher temperatures.

The single carbonyl band was completely removed from the spectrum at a lower temperature than the pair of bands. On silica (Fig. 4), the species giving the single band dominates the spectra at intermediate decomposition temperatures, whereas on alumina (Fig. 7) the species giving the pair of carbonyl bands is dominant.

The decomposition of adsorbed $Ir_4(CO)_{12}$ may be expected to involve, in the first place, replacement of carbonyl ligands in the coordination sphere of the iridium by surface hydroxyl groups of the support:

$$Ir_4(CO)_{12} + x\ SOH \rightarrow Ir_4(CO)_{12-x}(SOH)_x + x\ CO.$$

Similar ligand substitution reactions for the monometallic carbonyls $Mo(CO)_6$ and $W(CO)_6$ on alumina have been shown to be at least in part reversible (*38–41*). In the case of $Ir_4(CO)_{12}$, however, the spectrum of the adsorbed parent complex could not be restored by addition of CO following partial or complete decomposition, indicating that although ligand substitution may initiate the decomposition of adsorbed $Ir_4(CO)_{12}$, subsequent more drastic modification of the complex occurs which is irreversible. Two modes of irreversible decomposition may be proposed: fragmentation of the cluster into single iridium centers, or formation of larger metallic particles through aggregation of several Ir_4 clusters.

The infrared spectra obtained during activation of supported $Ir_4(CO)_{12}$ suggest that both types of decomposition process are occurring. The pair of carbonyl bands that disappear together are assigned to a dicarbonyl species $Ir(CO)_2$. Fragmentation of $Ir_4(CO)_{12}$ would initially produce four $Ir(CO)_3$ species. A pair of bands at 2086 and 2001 cm^{-1} for CO adsorbed in an IrY zeolite have been assigned to $Ir^I(CO)_3$ (*42*). The TPD curves for silica- and alumina-supported $Ir_4(CO)_{12}$ show, however, that there is substantial loss of CO over the temperature range in which the pair of carbonyl bands exist, so that a dicarbonyl species

formed by loss of CO from $Ir(CO)_3$ appears most likely. The dicarbonyl is the major species present on alumina after activation at 150°C, but not on silica. Stronger adsorption of cluster carbonyl complexes on alumina that on silica has been attributed to the more nucleophilic character of the hydroxyl groups on alumina (*5, 23*). This stronger support interaction on alumina is presumably also responsible for the greater extent of fragmentation of $Ir_4(CO)_{12}$.

The second mode of decomposition produces a single carbonyl band which shifts to lower frequency as CO is progressively removed. This behavior is identical to that observed during CO desorption from hydrogen-reduced catalysts, and similar frequency shifts have been reported during CO desorption from evaporated iridium films (*43*). The origin of the frequency shift is discussed further below; it is, however, characteristic of CO adsorbed on larger iridium clusters. These larger clusters are evidently produced at temperatures as low as 100°C, significantly below the decomposition temperature of bulk $Ir_4(CO)_{12}$ (*35*).

The TPD curves for both silica- and alumina-supported $Ir_4(CO)_{12}$ show production of CO_2 in two distinct steps, at around 160°C and above 300°C. The first CO_2 peak coincides exactly with the CO desorption peak, and probably results from a water-gas shift type of reaciton between CO and adsorbed water and/or surface hydroxyl groups. The quadrupole mass filter employed could not detect H_2, and attempts to detect D_2 desorption from an alumina-supported catalyst exchanged with D_2O were unsuccessful. The TPD curve for $Ir_4(CO)_{12}$–Al_2O_3 in flowing He reported by Hucul and Brenner (*26*) does show onset of H_2 evolution over the temperature range in which CO is desorbed, although these authors attribute all of the evolved H_2 to a redox reaction between the complex and surface hydroxyl groups. The desorption of CO_2 at high temperatures (above 300°C) is attributed to disproportionation of remaining CO ligands in this temperature range. Any surface carbon produced by this reaction is quite unreactive, since no CH_4 could be detected on subsequent treatment with H_2. It must be emphasized that the processes leading to CO_2 production do not play a major role in the overall chemistry of supported $Ir_4(CO)_{12}$, since the amounts of CO_2 evolved are quite small (less, in the case of Al_2O_3, than the CO_2 held by the support alone).

The following scheme summarizes the decomposition pathways proposed for $Ir_4(CO)_{12}$ on silica and alumina supports:

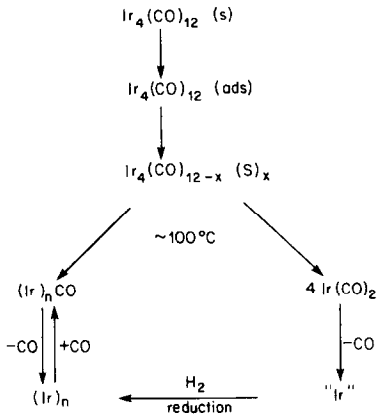

In this scheme (S) represents surface hydroxyl groups of the support which enter the iridium coordination sphere initiating fragmentation of the cluster. The nature of the species "Ir" and $(Ir)_n$ are discussed further below.

Characterization of the Silica-Supported Catalysts

The CO adsorption data in Table 1 show that catalysts prepared by decomposition of $Ir_4(CO)_{12}$ on silica *in vacuo* contain highly dispersed iridium. The CO : Ir ratios were only slightly increased by reducing in H_2, and the infrared spectra of adsorbed CO and TPD curves for CO desorption were quite similar for vacuum- and H_2-treated samples. Decomposition *in vacuo* evidently produces largely metallic iridium (denoted $(Ir)_n$ in the scheme above). The size of the iridium clusters cannot be determined from

the CO adsorption data since the stoichiometry of CO uptake is not known.

The spectrum of CO adsorbed on silica-supported iridium prepared from $Ir_4(CO)_{12}$ shows a single band which shifts to lower frequency as CO is desorbed. Similar variations of frequency with CO coverage were first reported for silica-supported platinum by Eischens and Pliskin (*44*), and have been seen more recently on single-crystal platinum (*45*) and palladium (*46*), as well as evaporated iridium films (*43*). Hammaker *et al.* (*47*) demonstrated using $^{13}CO/^{12}CO$ mixtures that coverage-dependent frequency shifts could be attributed to dipole–dipole interactions between adsorbed species, and further evidence for such interactions has been provided by several authors (*43, 48*). Regardless of the exact mechanism of the interaction, whether direct through-space dipole coupling or indirect vibrational coupling via the metal (*49, 50*), the observation of coverage-dependent frequency shifts for CO on the silica-supported iridium catalysts implies the existence of metal clusters containing more than 4 atoms. The magnitude of the total frequency shift, about 50 cm^{-1}, is significantly less than the 83-cm^{-1} shift reported by Reinalda and Ponec (*43*) for CO on evaporated iridium films. In the simplified model of Hammaker *et al.* (*47*), which assumes a two-dimensional layer of adsorbed CO molecules aligned parallel and bound perpendicularly to the surface, the frequency shift is proportional to the lattice sum $\Sigma 1/R_{ij}^3$, where R_{ij} is the distance between the centers of 2 dipoles i and j. For a square array, the lattice sum converges to within 5% of its limiting value after inclusion of approximately 100 dipoles. In this model, an array of at least 10 coupled dipoles would be needed to generate the observed frequency shift for CO adsorbed on silica-supported iridium. The model is in fact too approximate to allow the particle size to be deduced from the magnitude of the frequency shift, and there is no reason to believe that a single size of iridium cluster is produced by decomposition of $Ir_4(CO)_{12}$ on silica. Nevertheless, it may reasonably be concluded that the silica-supported catalysts contain iridium clusters in the size range 10–20 atoms, possibly in the form of two-dimensional rafts, which would maximize the possibility of dipole–dipole coupling in adsorbed CO molecules.

The TPD curves for CO adsorbed on silica-supported iridium (Fig. 2) provide further evidence for lateral interactions between adsorbed CO molecules. The influence of lateral interactions on the variation of heats of adsorption with coverage was first demonstrated by Wang (*49*). Since for nonactivated adsorption the heat of adsorption is approximately equal to the activation energy for desorption, the result of variation in heat of adsorption with coverage is a broadening of the TPD peak, and in extreme cases a splitting into several peaks (*50*). The curves in Fig. 2 do not show any clearly resolved splitting, but the 300°K width of the CO desorption peak may be attributed to the same interactions responsible for the vibrational coupling. Significant quantities of CO_2 were produced upon desorption of CO above 300°C, indicating that some dissociative desorption was occurring, but any carbon produced did not poison the subsequent readsorption of CO.

An anonymous referee has raised the suggestion that surface heterogeneity may be responsible for both the infrared frequency shifts and the breadth of the TPD curves. The effect of heterogeneity on the infrared spectra of adsorbed CO was first considered by Eischens and Pliskin (*44*), who showed that heterogeneity led to an increase in the number of bands due to adsorbed CO with increasing coverage, whereas a shift of a single band to higher frequency with increasing coverage was due to coupling between adjacent molecules. The spectra of CO on Ir–SiO_2 as a function of coverage (Fig. 5) clearly fall into the second category. The breadth of the TPD curves (300°C) certainly implies a

large difference in desorption energy between the CO molecules initially and finally desorbed (approximately 100 kJ mol^{-1}). Comparable differences (64 kJ mol^{-1}) have been reported, however, for CO desorption from a single-crystal Ir(110) surface (*56*). Nearest-neighbor repulsive interaction energies are typically of the order of only 20 kJ mol^{-1} (*50*), but dipolar coupling will extend over a much wider range. Thus although some contribution from surface heterogeneity cannot be discounted (particularly to the 40 to 50-cm^{-1} half-width of the infrared band), the major effect appears to be dipolar coupling.

The experiments with $^{12}CO:{}^{13}CO$ mixtures provide further support for the dipole interaction model. In the complete absence of coupling, adsorption of a 1:1 mixture would produce two bands of equal intensity, separated by about 46 cm^{-1}; the higher-frequency component corresponding to the single band observed with ^{12}CO at the same coverage. The effects of coupling are to lower the relative intensity of the low-frequency band, and to shift both bands to lower frequency (*48*). As the total surface coverage is reduced, these effects will diminish. The observed spectra show, at maximum surface coverage, a single band shifted by about 20 cm^{-1} relative to pure ^{12}CO, with an unresolved lower-frequency shoulder. As the surface coverage is reduced, the lower-frequency shoulder becomes more pronounced, and the spectrum approaches that expected for isolated species: a pair of bands of equal intensity at about 2020 and 1980 cm^{-1}.

The gravimetric adsorption data in Table 1 indicate that up to 30% of the iridium atoms in the highest-loading silica-supported catalysts are able to adsorb two CO molecules, although the infrared spectra show no clear evidence for the pair of carbonyl bands that might be expected for a dicarbonyl species. In the case of highly dispersed rhodium catalysts, for example, a pair of bands separated by 70 cm^{-1} (2096 and 2025 cm^{-1}) have been assigned to spatially isolated $Rh(CO)_2$ species (*57*). The frequency separation of the asymmetric and symmetric stretching modes of a dicarbonyl species depends on the magnitude of the interaction force constant. Using the simplified Cotton–Kraihanzel potential function (*51*), the interaction force constant for $Rh(CO)_2$ is estimated to be 0.6 mdyn $Å^{-1}$. The interaction force constant decreases with increasing coordinative saturation of the metal (*52*), and a smaller value would be expected for a dicarbonyl species formed on a metal atom belonging to a larger cluster. Given the 40 to 50-cm^{-1} half-width of the band due to CO adsorbed on $Ir–SiO_2$, a frequency separation of less than 50 cm^{-1} between the asymmetric and symmetric modes of an $Ir(CO)_2$ species (corresponding to an interaction force constant of less than about 0.4 mdyn $Å^{-1}$) would not be resolved. We thus suggest that the iridium atoms adsorbing two CO molecules are located at the edges or corners of iridium clusters, rather than being atomically dispersed. This mode should be contrasted with that proposed by McVicker *et al.* (*34*) for a highly dispersed conventional $Ir–Al_2O_3$ catalyst, in which a single 2060-cm^{-1} band was assigned to an atomically dispersed $Ir(CO)_2$ species in which the symmetric and asymmetric vibrations were only weakly coupled. The results for highly dispersed rhodium catalysts (*57*) make that assignment seem unlikely.

Characterization of the Alumina-Supported Catalysts

In contrast to the silica-supported catalysts, alumina-supported iridium samples prepared by decomposition of $Ir_4(CO)_{12}$ *in vacuo* adsorb substantially less CO than the corresponding hydrogen-reduced catalysts. These differences also show up in the infrared spectra of adsorbed CO, and in the TPD curves for CO desorption. The need to hydrogen reduce the catalysts following decomposition of the adsorbed complex *in vacuo* at 350°C in order to obtain maximum CO uptake suggests that partial oxidation of

the iridium is occurring during decomposition of $Ir_4(CO)_{12}$. The TPD data of Hucul and Brenner (*26*) show that hydrogen evolution as a result of oxidation of iridium of support hydroxyl groups begins above 200°C. The alumina used in (*26*) had been partially dehydroxylated; the extent of oxidation on the fully hydroxylated alumina used in this work may be somewhat greater.

The oxidation of the iridium appears to be associated with the fragmentation of $Ir_4(CO)_{12}$ into $Ir(CO)_2$ species during decomposition, since this is the dominant process on alumina. The further loss of CO from $Ir(CO)_2$ produces individual Ir atoms or ions which may penetrate into the support to form surface aluminates (*23*). These species do not chemisorb CO. According to this description, the extent of CO adsorption on an alumina-supported catalyst prepared by decomposition of $Ir_4(CO)_{12}$ *in vacuo* will depend on the relative contributions of the two decomposition pathways; formation of metallic clusters, or stronger interaction with the support to produce "oxidized" Ir species. The CO_2 produced during desorption of CO from vacuum-activated samples is attributed to partial removal of lattice oxygen atoms associated with the oxidized iridium.

Hydrogen reduction at 350°C produces metallic iridium with dispersions comparable to those obtained on the silica support. The infrared spectrum of CO adsorbed on the reduced catalysts is similar to that obtained on silica. The single band is broader than that observed on silica, and shows some evidence of higher- and lower-frequency shoulders which may be attributed to dicarbonayl species formed at the edges of iridium clusters. The dicarbonyl bands were better resolved on lower-iridium-loading samples. The frequency shift in the major band accompanying desorption is about 70 cm^{-1}, suggesting that the iridium clusters on alumina may be larger than those on silica. The spectrum obtained with a 1 : 1 ^{12}CO : ^{13}CO mixture (Fig. 6D) has the appearance expected for an array of coupled oscillators. The TPD curves for CO adsorbed on reduced iridium–alumina (Fig. 3) are also consistent with extensive CO : CO interactions. The increased half-width of the infrared band of adsorbed CO (60–70 cm^{-1} for $Ir-Al_2O_3$ compared with 40–50 cm^{-1} for $Ir-SiO_2$) does, however, suggest that surface heterogeneity may play a larger role in $Ir-Al_2O_3$ than in $Ir-SiO_2$.

Comparisons can be made with earlier data for the $Ir_4(CO)_{12}$-on-alumina system. In the previous infrared study (*6*), the spectral resolution was insufficient to allow the progressive shift in frequency of the adsorbed CO band with decreasing coverage to be seen, and a two-site model involving weakly and strongly held CO was proposed. The present work shows that model to be incorrect. There is in fact a distribution of adsorption strengths resulting from interactions between adsorbed CO molecules. The gravimetric CO adsorption data obtained here are in agreement with earlier volumetric adsorption results showing CO : Ir ratios greater than 1.0 for hydrogen-reduced catalysts (*5*). In the earlier work, attempts to observe iridium clusters on alumina by means of transmission electron microscopy (TEM) were unsuccessful, and it was concluded that the cluster size must be less than about 1.0 nm (*5, 7, 12*). If, however, the iridium clusters are in the form of two-dimensional rafts, as suggested from the magnitude of the frequency shifts of adsorbed CO with coverage, the clusters may be larger than 1.0 nm in diameter without being detected by TEM, due to insufficient contrast between the metal and the support (*54*).

Comparison with Conventional Catalysts

The most detailed information available on the chemisorption properties of conventional iridium–alumina catalysts is found in the recent paper by McVicker *et al.* (*34*). These authors prepared their catalysts by impregnation of the γ-alumina support with aqueous chloroiridic acid, followed by cal-

cination and reduction in hydrogen. Highly dispersed iridium was obtained, showing CO : Ir ratios as high as 1.7 (comparable with the maximum values obtained here). The infrared spectra of adsorbed CO showed bands at 2060 cm^{-1}, assigned to $Ir(CO)_2$ on sites of highest dispersion, and 2020 cm^{-1}, assigned to CO on larger crystallites. From the absence of measurable particles in TEM measurements, it was concluded that the highest-dispersion catalysts contained iridium crystallites less than 0.6 nm in diameter, and possibly single metal atom sites. Solymosi and Raskó (*33*) also observed two bands for CO adsorbed on a conventional iridium–alumina catalyst, with frequencies similar to those in (*34*), although their catalyst contained a considerably lower disperison of iridium (CO : Ir ratio 0.3). There is little information available on conventional iridium–silica catalysts. Guerra and Schulman (*30*) reported multiple infrared bands for CO adsorbed on iridium–silica prepared from ammonium hexachloroiridate, and suggested from surface area and TEM measurements that the iridium was in the form of thin clusters ranging from 20 Å in diameter and approaching monolayer thickness. Particle sizes in the 20-Å range for conventional iridium–silica catalysts have also been reported by Foger and Anderson (*12*), and by Wang and Schmidt (*53*).

The silica- and alumina-supported catalysts prepared from $Ir_4(CO)_{12}$ have dispersions (as measured by CO uptake) as high as the most highly dispersed conventional catalysts. The infrared spectra of adsorbed CO are, however, significantly different from those reported for the conventional catalysts. In particular, the coverage-dependent frequency shifts suggest that the morphology of the iridium clusters in the catalysts derived from $Ir_4(CO)_{12}$ is different from that found in catalysts prepared from hexachloroiridic acid. Further investigation is needed to establish the reasons for these differences; the absence of a high-temperature calcination step and of chlorine in the carbonyl complex preparations may be suggested as possibilities.

ACKNOWLEDGMENT

This work was supported by Grant CHE 77-20373 from the National Science Foundation.

REFERENCES

1. Anderson, J. R., and Mainwaring, D. E., *J. Catal.* **35,** 162 (1974).
2. Robertston, J., and Webb, G., *Proc. R. Soc. London Ser. A* **341,** 383 (1974).
3. Smith, G. C., Chojnacki, T. P., Dasgupta, S. R., Iwatate, K., and Watters, K. L., *Inorg. Chem.* **14,** 1419 (1975).
4. Ichikawa, M., *J. Chem. Soc. Chem. Commun.*, 26 (1976).
5. Anderson, J. R., Elmes, P. S., Howe, R. F., and Mainwaring, D. E., *J. Catal.* **50,** 508 (1977).
6. Howe, R. F., *J. Catal.* **50,** 196 (1977).
7. Anderson, J. R., and Howe, R. F., *Nature* **268,** 129 (1977).
8. Smith, A. K., Theolier, A., Basset, J. M., Ugo, R., Commereuc, D., and Chauvin, Y., *J. Amer. Chem. Soc.* **100,** 2590 (1978).
9. Brenner, A., *J. Chem. Soc. Chem. Commun.*, 251 (1979).
10. Ichikawa, M., *J. Catal.* **56,** 127 (1979).
11. Ichikawa, M., *J. Catal.* **59,** 67 (1979).
12. Foger, K., and Anderson, J. R., *J. Catal.* **59,** 325 (1979).
13. Ballivet-Tkatchenko, D., and Coudurier, G., *Inorg. Chem.* **18,** 558 (1979).
14. Gelin, P., Ben Taarit, Y., and Naccache, C., *J. Catal.* **59,** 357 (1979).
15. Smith, A. K., Hugues, F., Theolier, A., Basset, J. M., Ugo, R., Zandereghi, G. M., Bilhou, J. L., Bilhou-Bougnol, V., and Graydon, W. F., *Inorg. Chem.* **18,** 3105 (1979).
16. Vanhove, D., Makambo, L., and Blanchard, M., *J. Chem. Res. Synop.*, 335 (1980).
17. Bowser, W. M., and Weinberg, W. H., *J. Amer. Chem. Soc.* **102,** 4720 (1980).
18. McVicker, G. B., and Vannice, M. A., *J. Catal.* **63,** 25 (1980).
19. Watters, K. L., Howe, R. F., Chojnacki, T. P., Fu, C. M., Scheider, R. L., and Wong, N. B., *J. Catal.* **66,** 424 (1980).
20. Guczi, L., Schay, Z., Matusek, K., Bogyay, I., and Steffler, G., *in* "Proceedings, 7th International Congress on Catalysis, Tokyo, 1980," paper A12.
21. Hugues, F., Bussiere, P., Basset, J. M., Commereuc, D., Chauvin, Y., Bonneviot, L., and Olivier, D., *in* "Proceedings, 7th International Congress on Catalysis, Tokyo, 1980," paper A28.
22. Ichikawa, M., and Shikakura, K., *in* "Proceedings, 7th International Congress on Catalysis, Tokyo, 1980," paper B17.

23. Kuznetsov, V. L., Bell, A. T., and Ermakov, Y. I., *J. Catal.* **65,** 374 (1980).
24. Besson, B., Moraweck, B., Smith, A. K., Basset, J. M., Psaro, R., Fusi, A., and Ugo, R., *J. Chem. Soc. Chem. Commun.*, 569 (1980).
25. Watson, P. L., and Schrader, G. L., *J. Mol. Catal.* **9,** 129 (1980).
26. Hucul, D. A., and Brenner, A., *J. Amer. Chem. Soc.* **103,** 217 (1981).
27. Deeba, M., and Gates, B. C., *J. Catal.* **67,** 303 (1981).
28. Hucul, D. A., and Brenner, A., *J. Phys. Chem.* **85,** 496 (1981).
29. Lynds, L., *Spectrochim. Acta* **20,** 1369 (1964).
30. Guerra, C. R., and Schulman, J. H., *Surf. Sci.* **7,** 229 (1967).
31. Falconer, J. L., Wentrcek, P. R., and Wise, H., *J. Catal.* **45,** 248 (1976).
32. Fiedorow, R. M. J., Chahar, B. S., and Wanke, S. E., *J. Catal.* **51,** 193 (1978).
33. Solymosi, F., and Raskó, J., *J. Catal.* **62,** 253 (1980).
34. McVicker, G. B., Baker, R. T. K., Garten, R. L., and Kugler, E. L., *J. Catal.* **65,** 207 (1980).
35. Psaro, R., Fusi, A., Ugo, R., Basset, J. M., Smith, A. K., and Hugues, F., *J. Mol. Catal.* **7,** 511 (1980).
36. Abel, E. W., Hendra, P. J., Mclean, R. A. N., and Qurashi, M., *Inorg. Chim. Acta* **3,** 77 (1969).
37. Price, W. C., and Tetlow, K. S., *J. Chem. Phys.* **16,** 1157 (1948).
38. Brenner, A., and Burwell, R. L., *J. Amer. Chem. Soc.* **97,** 2565 (1975).
39. Howe, R. F., *Inorg. Chem.* **15,** 486 (1976).
40. Brenner, A., and Hucul, D. A., *J. Catal.* **61,** 216 (1980).
41. Kazusaka, A., and Howe, R. F., *J. Mol. Catal.* **9,** 183, 199 (1980).
42. Gelin, P., Ben Taarit, Y., and Naccache, C., *in* "Proceedings, 7th International Congress on Catalysis, Tokyo, 1980," paper B15.
43. Reinalda, D., and Ponec, V., *Surf. Sci.* **91,** 113 (1979).
44. Eischens, R. P., and Pliskin, W. A., *in* "Advances in Catalysis and Related Subjects," Vol. 10, p. 1. Academic Press, New York/London, 1958.
45. Shigeishi, R. A., and King, D. A., *Surf. Sci.* **58,** 379 (1976).
46. Bradshaw, A. M., and Hoffman, F. M., *Surf. Sci.* **72,** 513 (1978).
47. Hammaker, R. A., Francis, S. A., and Eischens, R. P., *Spectrochim. Acta* **21,** 1295 (1965).
48. Crossley, A., and King, D. A., *Surf. Sci.* **68,** 528 (1977).
49. Wang, J. S., *Proc. R. Soc. London Ser. A* **161,** 127 (1937).
50. King, D. A., *CRC Crit. Rev. Solid State Mater. Sci.* **7,** 167 (1978).
51. Cotton, F. A., and Kraihanzel, C. S., *J. Amer. Chem. Soc.* **84,** 4432 (1962).
52. Moskovits, M., and Hulse, J. E., *Surf. Sci.* **78,** 397 (1978).
53. Wang, T., and Schmidt, L. D., *J. Catal.* **66,** 301 (1980).
54. Yacaman, M. J., and Dominquez, J. M., *J. Catal.* **67,** 475 (1981).
55. Bailey, D. C., and Langer, S. H., *Chem. Rev.* **81,** 110 (1981).
56. Taylor, J. L., Ibbotson, D. E., and Weinberg, W. H., *J. Chem. Phys.* **62,** 4652 (1975).
57. Cavanagh, R. R., and Yates, J. T., *J. Chem. Phys.* **74,** 4150 (1981).